LLNL-CONF-656184

LAWRENCE LIVERMORE NATIONAL LABORATORY

Investigating Shock Initiation and Detonation in Powder HMX with Reactive Mesoscale Simulations

H. K. Springer, K. S. Vandersall, C. M. Tarver, P. S. Souers

June 30, 2014

15th International Detonation Symposium
San Francisco, CA, United States
July 13, 2014 through July 18, 2014

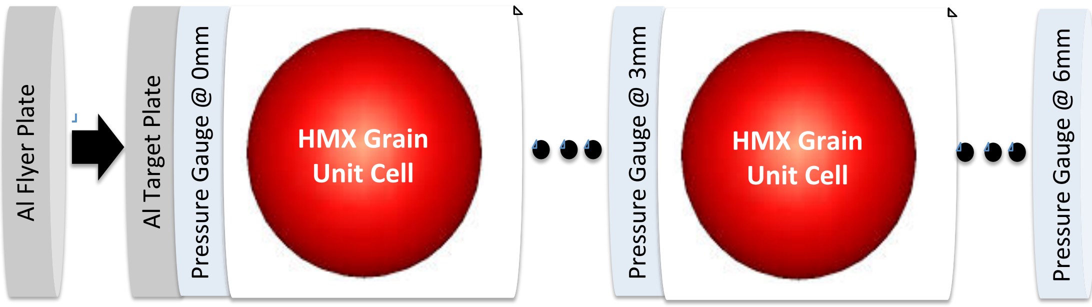

Fig. 1. Row of HMX grain unit cell geometry used in shock initiation simulations. Shock loading is realized with the aluminum flyer impacting the aluminum target plate. Steady-state detonation simulations also employ a unit cell representation but the pressure gauges are removed and the plates are replaced by a high-pressure boundary condition to achieve transition to detonation. Figure not shown to scale.

Results & Discussion

Shock Initiation Response of HMX Powder

Figure 2 shows the in situ pressure gauge measurements[2] at 0, 3, and 6 mm positions for a ~1.24 g/cc (ϕ_{HMX}~0.65) HMX powder impacted by an aluminum flyer plate at 477 m/s corresponding to a 1.3 GPa input pressure. Modeling predictions are shown for the baseline case of ϕ_{HMX}=0.65, r_{HMX}=2.5μm (spherical grains), and n=0. While the time-of-arrival (TOA) predictions and peak pressures slightly deviate from data for the 3 mm gauge, these results are promising. Early predicted TOA at the 3 mm gauge may result from relatively fast chemical kinetics or an unreacted EOS that is relatively stiff.

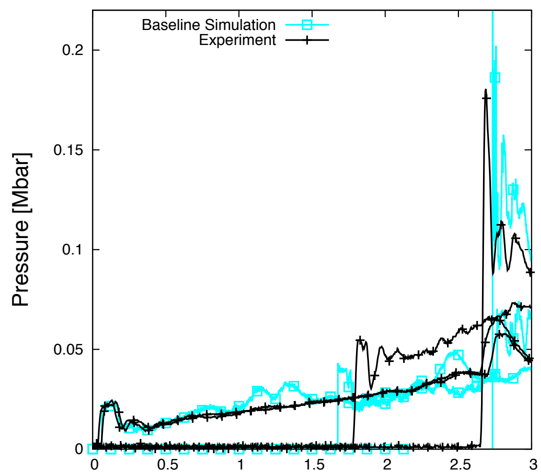

Fig. 2. In situ pressure gauge measurements[2] at 0, 3, and 6 mm positions (three black curves) for ~1.24 g/cc HMX powder impacted at 1.3 GPa. Modeling predictions are shown for the baseline case of ϕ_{HMX}=0.65 and n=0 (three cyan curves).

Figure 3 shows the reaction evolution in our mesoscale simulations after transition to detonation for the baseline case (ϕ_{HMX}=0.65, n=0, r_{HMX}=2.5μm, spherical grains). In contrast to more conventional shock initiation in high density heterogeneous explosives, where burning initiates at inner hot spots from pore collapse and progresses outwards, our simulations suggest a different mode. For our study on low density powder explosives, the product gases are observed to jet into the outer pore regions, engulfing HMX grains in gas, and burning progresses from the outside in. From our calculations, we estimate the distance between the reaction front and the point of nearly complete reaction to be ~10 unit cell lengths.

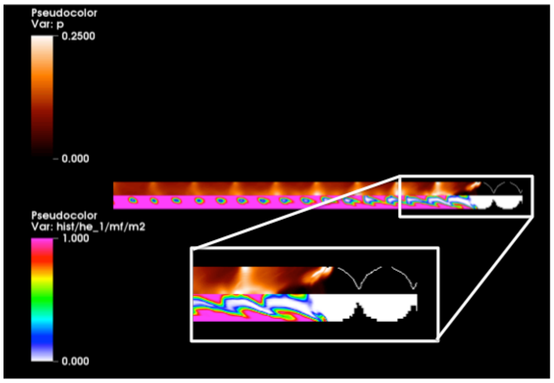

Fig. 3. Reaction evolution in HMX grain unit cell calculations in baseline case. Pressure (Mbar) is shown at the top and mass fraction reacted is shown at the bottom.

We conduct a perturbation study to probe the effects of slight model parameter variations from baseline values for a constant input pressure of 1.3 GPa. Figure 4 shows the in situ pressure gauge predictions for increases in kinetics and porosity, as well as switching to a Cheetah-based product EOS. Shock sensitivity increases significantly with increased kinetic model parameter (n=0.1 from baseline 0.0) and porosity (ϕ_{HMX}=0.60 from baseline 0.65) but using the Cheetah EOS had less impact. For increases in porosity and kinetics, TOA predictions at the 3 mm and 6 mm gauges are much earlier than the experiments. Also, the peak pressure predictions for the 3 mm gauge is consistent with a detonation, implying a run distance of less than 3 mm.

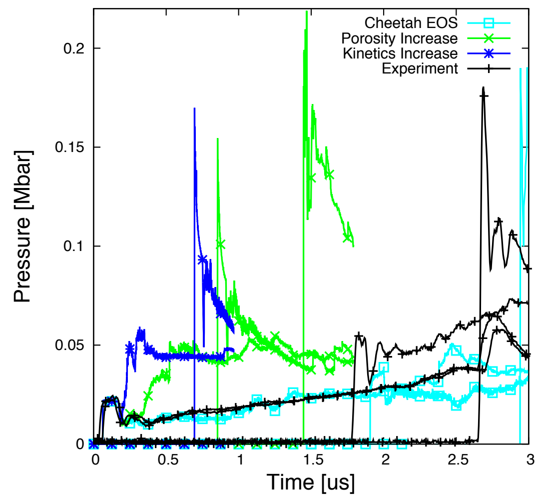

Fig. 4. Model predictions of in situ pressure gauge response for increases in kinetics (n=0.1) (blue curves) and porosity (ϕ_{HMX}=0.60) (green curves), as well as switching to a Cheetah-based product EOS (cyan curves). Experimental results[2] are shown for comparison (black curves).

We conduct an additional study probing changes to the HMX grain shape for a constant volume fraction (ϕ_{HMX}=0.65) and input pressure (1.3 GPa). Figure 5 shows the in situ pressure gauge predictions for ellipsoidal HMX grains with major axis oriented parallel (prolate spheroid, or "cigars") and perpendicular (oblate spheroid, or "discs") to the simulation axis-of-symmetry. The simulation axis-of-symmetry, itself, is parallel to the shock direction. The ratio of the major axis to the minor axis is 3:1 and the minor axis size is equal to the baseline spherical grain radius (r_{HMX}=2.5μm). Shock sensitivity increased significantly with the cigar grains but decreased with the disc grains. For the cigar grains, TOA prediction at the 3 mm gauge is much earlier than the experiments. Also, peak pressure prediction for the 3 mm gauge is consistent with a detonation, implying a run distance of less than 3 mm. In contrast, the reaction in the disc grains is not observed to transition to a detonation by 3 mm.

Increases in shock sensitivity with the cigar grains is unexpected since recent calculations[27] for elliptical pores suggest that peak hotspot temperatures are higher when the shock direction is perpendicular to the ellipse major axis rather than parallel to it. However, our study employs 2D axisymmetric calculations with repeating elliptical grains (1000s of grains), whereas the other calculations are for single isolated pores under 2D plane strain conditions. These different approaches must be reconciled with the experiments being simulated.

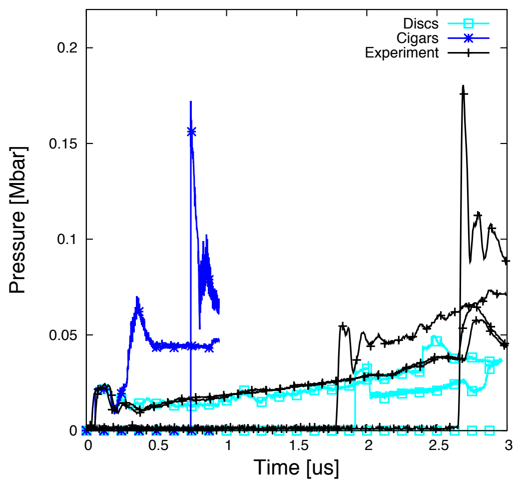

Fig. 5. Model predictions of in situ pressure gauge response for ellipsoidal HMX grains with major axis oriented parallel to the shock direction ("cigars", cyan curves) and perpendicular to the shock direction ("discs", blue curves). Experimental results[2] are shown for comparison (black curves).

Steady-State Detonation of HMX Powder

It is important for these mesoscale modeling approaches to not only capture the shock initiation response but also the subsequent steady-state detonation phase of low density materials. Detonation theory contends that the product EOS, initial density, and chemical energy released define the detonation velocity (V_{det}) at the macroscale in explosives. We perform simulations studying the influence of solid HMX fraction (ϕ_{HMX}) on the V_{det} for two different product EOS. Experimental V_{det} measurements of HMX powder over a range of densities[20] are used to benchmark model predictions.

Figure 6 shows V_{det} predictions in HMX powder as a function of ϕ_{HMX} for the baseline experimental-based and Cheetah-based product EOS. For all cases, V_{det} predictions increase with increasing ϕ_{HMX}, similar to experimental data, but there is a notable change in slope at ϕ_{HMX} > 0.45-0.55. For ϕ_{HMX} = 0.5-0.65, V_{det} predictions for the baseline and the Cheetah-based product EOS are consistently lower than data. This suggests that the detonation may not have reached steady-state conditions in these higher ϕ_{HMX} simulations. The relatively higher V_{det} predictions for the Cheetah-based product EOS are expected since its associated CJ detonation velocity at crystal density is slightly higher than that for the experimentally-based product EOS.

In contrast, V_{det} predictions are consistent with experimental data for ϕ_{HMX} = 0.35-0.4. Based on earlier results in this study, we expect that the shock initiation occurs more rapidly at lower densities, culminating to a steady-state detonation in the simulation. Overall, these results suggest that simulation domains must be sufficiently long to ensure steady-state detonation conditions are achieved over the range of densities studied.

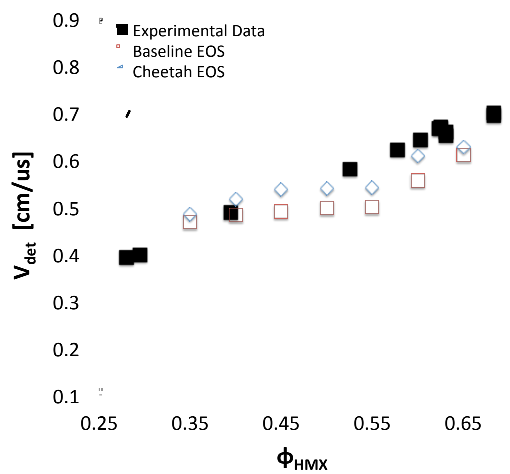

Fig. 6. V_{det} predictions in HMX powder as a function of ϕ_{HMX} for baseline experimentally-based product EOS (red boxes) and Cheetah-based product EOS (blue diamonds). Experimental measurements[20] of steady-state detonation on HMX powder is shown for comparison (black boxes and fitted line).

Conclusions

Preliminary experimental benchmarking of our mesoscale simulations is promising. Simulations capture detailed in situ pressure gauge response during shock initiation and $V_{det}(\phi_{HMX})$ trends during detonation for low density material using simplified material models and a unit cell (row) representation of HMX grains. Perturbation studies demonstrate the strong influence of porosity, kinetics, and cigar-shaped grains on shock sensitivity.

Mesoscale simulations demonstrate better agreement with steady-state detonation data at lower densities (ϕ_{HMX} = 0.35-0.4), where materials initiate more rapidly, than at higher densities ($\phi_{HMX} \geq 0.45$). These results suggest that simulation domains must be sufficiently long to ensure steady-state detonation conditions are achieved over the range of densities studied.

Further experimental validation of mesoscale modeling approaches is necessary before we can confidently use predictions. In the near-term, modeling must be validated to shock initiation experiments over a wider range of HMX powder densities and input shock pressures than those considered in this study. These studies should investigate the effect of using a variable HMX grain size distribution, different unreacted EOS, and a temperature-dependent heat capacity. In the long-term, we need temporally- and spatially-resolved temperature, deformation, and pressure data for single and multiple pores subjected to a range of shock pressures to compare to closely-coupled simulations. Considering the heterogeneity of energetic materials, the relevant length-scales of hotspots and the time-scales of pore collapse, this is most certainly a daunting experimental challenge.

There are several near-term benefits to these studies. The ability to predict in situ pressure gauge response is valuable because it can be directly used to parameterize existing reactive flow models, such as Ignition & Growth (I&G)[28]; in turn, the I&G model can be used for system-scale hazard assessments. Also, our emerging understanding of microstructure-shock response, including porosity and grain shape effects, can be used to guide the design of new energetic material microstructures and novel additive manufacturing techniques.

Our longer-term goal is to use mesoscale modeling as the basis for developing advanced continuum-scale models that incorporate basic structure-property information and hot spot mechanisms. Since future model parameters will be more closely coupled to experimental characterization data, calibration is more straightforward and less non-unique. Such models will enable tailoring of explosive type and microstructure for specific applications in order to optimize both performance and safety. Future models will also enable sensitivity studies to identify the most important parameters and propagate associated uncertainties, based on small-scale experiments, to system-scale for quantification of margins and uncertainties.

Acknowledgements

This work was performed under the auspices of the U.S. DOE by LLNL under Contract DE-AC52-07NA27344. This research was supported by the Joint DoD-DOE Munitions Technology Development Program. We acknowledge the support of Sorin Bastea with the Cheetah calculations for HMX powder detonation velocities. LLNL Technical Report, LLNL-CONF-656184.

References

1. Sheffield, S.A., Gustavsen, R.L., and Anderson, M.U., "Chapter 2: Shock Loading of Porous High Explosives" in *High-Pressure Shock Compression of Solids IV* edited by Davidson, L., Horie, Y., and Shahinpoor, M., Springer-Verlag, New York, 1997.

2. Garcia, F., et al, "Shock initiation experiments with ignition and growth modeling on low density HMX", *AIP Conf. Proc.,* **500**, p 052048-1, 2014.

3. Urtiew, P.A., et al, "Shock sensitivity of LX-04 containing delta phase HMX at elevated temperatures", *AIP Conf. Proc.,* **706,** p 1053, 2004.

4. Green, L. G., et al, “Delayed detonation in propellants from low velocity impact”, *Proc. 7th Int. Det. Symp.*, p 256, 1981.

5. Finnegan, S.A. et al, “ Impact-induced delayed detonation in an energetic material debris bubble formed at an air gap”, *Int. J. Impact Engr.,* **14**, p 241, 1993.

6. Haskins, P.J., et al, “An investigation of XDT events in the projectile impact of secondary explosives”, *Proc. 10th Int. Det. Symp.*, p 148, 1993.

7. Cook, M.D. and Haskins, P.J., “Fragment impact of energetic materials- A review of experimental studies and an analysis of reaction mechanisms”, *Proc. 14th Int. Det. Symp.*, p 591, 2010.

8. McAfee, J.M., “Chapter 8: The Deflagration-to-Detonation Transition” in *Non-Shock Initiation of Explosives* edited by B. W. Asay, Springer-Verlag, New York, 2010.

9. Baer, M.R., et al, “Micromechanical modeling of heterogeneous energetic materials” *Proc. 11th Int. Det. Symp.*, p 788, 1998.

10. Menikoff, R., “Granular explosives and initiation sensitivity” *LANL Technical Report, LA-UR-99-6023,* 1999.

11. Baer, M.R., “Modeling heterogeneous energetic materials at the mesoscale” *Thermochemica Acta,* **384**, p 351, 2002.

12. Barton, N.R., et al, “Defect evolution and pore collapse in crystalline energetic materials” *Modeling Simul. Mater. Sci. Eng.,* **17,** p 035003-1, 2009.

13. Panchadhara, R. and Gonthier, K.A., “Mesoscale analysis of volumetric and surface dissipation in granular explosive induced by uniaxial deformation waves,” Shock Waves, **21**, p 43, 2011.

14. Reaugh, J.E., “Grain-scale dynamics in explosives” *LLNL Technical Report, UCRL-ID-150388,* 2002.

15. Mader, C.L., “Numerical modeling of explosives and propellants”, 3rd Ed. (Boca Raton, FL:CRC Press), 2008.

16. Fried, L.E., et al, “The role of viscosity in TATB hot spot ignition” *AIP Conf. Proc.,* **1426,** p 299, 2012.

17. Springer, H.K., et al, “Mesoscale modeling of deflagration-induced deconsolidation in polymer-bonded explosives”, *AIP Conf. Proc.,* **1426,** p 705, 2012.

18. Springer, H.K., et al, “Investigating short-pulse shock initiation in HMX-based explosives with reactive meso-scale simulations”, *AIP Conf. Proc.,* **500,** p 052041-1, 2014.

19. Welle, E.J., et al, “Microstructural effects on the ignition behavior of HMX”, *AIP Conf. Proc.,* **500,** p 052049-1, 2014.

20. Steinberg, D.J., “Comparison of Experimental Data on Detonation Velocity and Chapman-Jouguet Pressure vs Initial HE density with Predictions from Ree’s Model Equation of State,” *Proc. 8th Int. Det. Symp.*, p 513, 1985.

21. Nichols, A.L., “ALE3D User’s Manual, Version 4.18” *LLNL Technical Report, LLNL-SM-604812,* 2012.

22. Olinger, B., et al, “The linear and volume compression of beta-HMX and RDX to 9 GPa” *Proc. Symp. (Int.) on High Dynamic Pressures,* p 3 1979.

23. Henson, B.F., et al, “Evidence for thermal equilibrium in the detonation of HMX” *Proc. 12th Int. Det. Symp.*, p 987, 2002.

24. Menikoff, R., et al, “Analysis of wave profiles for single-crystal cyclotetramethylene

tetranitramine" *J. Appl. Phys.,* **97,** p 023529-1, 2005.

25. Vandersall, K.S., Tarver, C.M., Garcia, F., and Chidester, S.K., "On the low pressure shock initiation of octahydro-1,3,5,7-tetranitro-1,3,5,7-tetrazocine based plastic bonded explosives", *J. Appl. Phys.,* **107,** p 094906-1, 2010.

26. Steinberg, D.J., "Equation of State and Strength Properties of Selected Materials" *LLNL Technical Report, UCRL-MA-106439* Change 1 1996.

27. Damm, D.L., et al, "Development of a grain scale model for initiation of HNS" *Submitted to the Proc. 15th Int. Det. Symp.*, 2014.

28. Lee, E.L. and Tarver, C.M., "Phenomenological model of shock initiation in heterogeneous explosives", *Phys. Fluids*, **23**, p 2362, 1980.